Journal of the European Ceramic Society 20 (2000) 1845–1851

Fundamental parameters approach in the Rietveld method: a study of the stability of results versus the accuracy of the instrumental profile

A.L. Ortiz [a,1], F.L. Cumbrera [a], F. Sánchez-Bajo [b,*], F. Guiberteau [b], R. Caruso [b,2]

[a] *Departamento de Física, Facultad de Ciencias, Universidad de Extremadura, Ctra de Elvas s/n, 06071 Badajoz, Spain*
[b] *Departamento de Electrónica e Ingeniería Electromecánica, Escuela de Ingenierías Industriales, Universidad de Extremadura, Ctra de Elvas s/n, 06071 Badajoz, Spain*

Received 7 October 1999; received in revised form 14 February 2000; accepted 17 February 2000

Abstract

The Rietveld refinement method is a valuable tool for structural and microstructural analysis of a variety of crystalline materials. In spite of many important developments in the last decade, most current Rietveld programs suffer from a number of drawbacks. In order to overcome these disadvantages, the ''fundamental parameter approach'' (FPA) has been used recently. The FPA uses a convolution-based method to build up X-ray line profiles. Instrumental and sample aberrations are calculated from first principles, and convoluted with the emission profile to form the final line profile. Although this methodology eliminates the need for a standard, in practice some instrumental parameters must be refined, resulting in certain empiricism in this procedure. Therefore, the comparison with a strain-free and 'infinite crystallite size' standard becomes necessary. In this work we have performed a study of the stability of quantitative analysis and microstructural results versus simulated inaccurate instrumental profiles. All the FPA calculations were performed on X-ray diffraction data from a technologically attractive and scientifically challenging system: liquid-phase-sintered SiC (LPS SiC).

Keywords: SiC; Sintering; X-ray methods

1. Introduction

X-ray powder diffraction (XRD) is perhaps the most useful analytical method for obtaining quantitative and microstructural phase information from multicomponent mixtures.[1] However, some advanced ceramics exist in a number of different polytypic forms, sharing nearly the same lattice spacings but with different crystal symmetries. In this case, the quantitative analysis is difficult because of the significant overlap of the Bragg reflections from the polytypes, making traditional quantitative X-ray diffraction methods unsatisfactory.[2,3] It is well recognized that the use of the Rietveld method[4,5] has many advantages:[6]

- whereas traditional procedures make use of selected individual reflections in order to estimate the weight fractions, in the Rietveld method all reflections for each phase are included in the fit, then minimizing the problem of overlapped peaks;
- in the techniques that use integrated intensities of individual peaks, the presence of preferred orientation effects[7,8] constitutes a serious drawback to obtain reliable results in quantitative analysis. However, in the Rietveld method the texture effects can be considered in the fitting process, leading to a more accurate estimation of relative phase proportions;
- in addition, the amount of information that we need for quantitative analysis in the Rietveld method is small and is related to the crystal structure of the phases, precluding the need for a standard.

* Corresponding author.
[1] Now at Department of Metallurgy and Materials Engineering, Institute of Materials Science, University of Connecticut, Storrs, CT 06269, USA.
[2] CONICET Member, Laboratorio de Materiales Cerámicos IFIR-CONICET, Universidad Nacional de Rosario, Avda Pellegrini 250, 2000, Rosario, Argentina.

0955-2219/00/$ - see front matter
PII: S0955-2219(00)00056-X

So far, several Rietveld codes have been reported in the literature, i.e. FULLPROF,[9] GSAS,[10] RIETAN,[11] etc., and sometimes the spread and the reproducibility of their results have been evaluated for a number of materials and round-robins.[12,13] The parameters that are usually refined are of two kinds: structural and profile. It is well known that refinement of these last parameters has many drawbacks, i.e. those related with negative values for the squared full width of maxima when dealing with Caglioti's parameters.[14] Therefore, there is a need to develop better and more robust algorithms which improve the numerical stability of the refinements.

In this regard, the BGMN code[15] can be ascribed to a new generation of Rietveld programs which are referred to as 'fundamental parameters approach to profile analysis of powder data' (FPA). Another Rietveld code which also incorporates this new philosophy is KOALARIET.[16] In fact, BGMN has some features which are not commonly found in other Rietveld programs, namely:

- numerical algorithms which guarantee stability;
- automatic calculation without the necessity for a refinement strategy influenced by the user;
- automatic correction of preferred orientation with spherical harmonics; thus multiple preferred orientations are allowed;
- a peak model which has a physical basis is used, eliminating the use of traditional U, V and W parameters, which have little physical meaning.

With regard to this last point, each Bragg reflection is individually as a result of three factors: (a) the spectral distribution of the X-ray source, (b) the geometrical conditions of the experiment, and (c) the microstructural features of the sample (crystallite size and microstrain effects). In fact, BGMN separates points (a) and (b) as a prior task to the Rietveld refinement.[17] Thus, the wavelength distribution is experimentally determined and described by the sum of four Lorentzian functions. On the other hand, the geometric function is evaluated by ray tracing (Monte-Carlo simulation) concerning all dimensions of the diffractometer (collimator, focus and slit dimensions, goniometer radius, etc.). This profile is simulated at different 2θ intervals and described by the sum of several squared Lorentzian functions. The parameters of these functions are subsequently interpolated over the entire angular range and these profiles are convoluted afterwards with the spectral distribution. The physical parameters of the diffractometer are measurable quantities which are not refined usually but may be required. This latter becomes necessary, as in practice, one would not expect to obtain refined values matching the actual diffractometer values exactly; on the other hand, there are too many second order effects in diffractometer profiles and some instrumental effects cannot be described accurately enough to make this feasible.

Finally, the parameters describing the crystallite size and microstrain are introduced as refinable values within the Rietveld refinement. In this way, the difficulty and intractability of conventional line-broadening methods[18–24] are overcome and crystallite size can be readily obtained for a specific lattice direction.

The purpose of this paper is to assess the performance and stability of the BGMN Rietveld results (quantitative analysis and crystallite size determination) versus the degree of accuracy in modelling the instrumental component of the profile. Another interest of this work concerns the material employed for the test: a liquid-phase-sintered SiC (LPS SiC) ceramic. This class of ceramics has recently attracted interest because one can pressureless-sinter these materials to near-full densities at lower temperatures (1850 to 1950°C) relative to solid-state sintering.[25–27] A particularly important aspect of this class of materials is that they can be significantly toughened through careful microstructure design, wherein elongated SiC grain-reinforcements are grown in situ during sintering.[28] The elongate nature of the SiC grains and the weakness at the grain boundaries promote crack-wake bridging in these ceramics, resulting in a significant increase in the toughness.[28–31] However, the study of LPS SiC ceramics by using XRD is very complex because pure SiC can exist in several different polytypic forms which are all close-packed structures, but consist of distinct periodic combinations of hexagonal and cubic stacking sequences.[†] Thus, although LPS SiC ceramics represent a new class of potentially important structural materials, the evolution of their microstructures remain poorly understood. Then, the present study is also a contribution towards the broad understanding of microstructural evolution in LPS SiC.

2. Experimental procedure

Commercially available sub-micron powders of β-SiC (BF-12, H.C. Starck, Germany), Y_2O_3 (Fine grade, H.C. Starck, Germany) and Al_2O_3 (AKP-30, Sumitomo Chemicals, Japan) have been used as starting powders. The composition of the batch is given in Table 1. The details of the processing are described in Ref. 28. The sample was isothermally sintered in a graphite furnace (Astro Industry, Santa Rosa, CA) at 1950°C for 1 h

[†] The different stacking sequences can be described by the Ramsdell notation,[32] which is used for distinguishing the different polytypes. In this notation, the symbol nS refers to a polytype with n number of Si–C layers along the *c*-axis of an equivalent hexagonal unit cell, and S refers to the cell symmetry, i.e. either cubic (C), hexagonal (H) or rhombohedral (R). The cubic form of SiC (3C) is referred to as β-SiC, and all the others are collectively referred to as α-SiC.

Table 1
Composition of the starting powders before sintering

Powder	Mass (%)
β-SiC	73.86
Y_2O_3	14.92
Al_2O_3	11.22

with a flowing argon atmosphere. After removing it from the furnace, the sample was crushed in a mortar and pestle to obtain a powder for X-ray characterization.

The X-ray diffraction patterns of the LPS SiC sample were obtained with a Philips PW-1800 powder diffractometer employing CuK_α radiation ($\lambda = 1.54183$ Å) and a graphite monochromator. The generator settings were 40 KV and 35 mA. The diffraction data were collected from 20 to 95° 2θ with a step width of 0.05° and a counting time of 5 s per step. Likewise, an α-Al_2O_3 powder specimen was recorded using the same experimental conditions. This specimen was well-annealed and sieved with grain size greater than 53 μm in order to have a standard where the peak shifts and broadening come only from spectral and instrumental effects.

3. Methodology

In a first step, the ray tracing algorithm models the instrumental profiles at discrete 2θ angles. An interpolation is necessary afterwards to construct a file for subsequent Rietveld refinements. At this point complete knowledge of the following geometrical aspects concerning the diffractometer is crucial: radius of the goniometer, dimensions of the divergence and receiving slits, focus and collimators, distance of the secondary monochromator to the sample, etc. On the other hand, we must consider the global characteristics of the experiment: transmission, reflection or capillary geometry. Most of these features are dependent on the factory settings on the instrument. For any practical case, the following question is raised: how to estimate for the percentage of empiricism in the definition of the instrumental function? Note that elimination of any empiricism in the definition of this function cannot be realized. Therefore, we need qualitative and quantitative assessment of the agreement between the modelled instrumental profile and that measured on a standard. Special attention will be devoted in this work to study the influence of a slight departure from the true instrumental function on both quantitative analysis of the phases and crystallite size measurements.

Starting with the geometrical data supplied by the manufacturer, and after fitting this data with subsequent convolution with the spectral distribution, we obtained excellent agreement between the calculated instrumental peaks and those of the standard (see Fig. 1). Before proceeding to the corresponding Rietveld refinement, we have intentionally distorted the accurate instrumental function by modifying slightly the goniometer radius; thus, we have obtained two smeared instrumental peaks, narrower and wider than the true one (Table 2 and Fig. 1). At this stage we performed the three Rietveld calculations by assuming alternatively each one among the three above mentioned instrumental functions. The following parameters were refined:

- the background, which was modelled as a polynomial function,
- the scale factors,
- the global instrumental parameters (zero-point 2θ shift and systematic shifts, depending on transparency and off-centering sample),
- the lattice parameters for all phases,
- preferred orientation effects, which were evaluated by using spherical harmonics functions of even order. It has been proved[33] that the consideration of preferred orientation effects is not only important with the aim of improving the refinement but also indispensable to obtain the accurate proportion of the phases.

4. Results and discussion

A careful visual examination of the diffractogram (Fig. 2) clearly shows that the LPS SiC sample contains α-SiC (6H and 4H) and YAG ($Y_3Al_5O_{12}$) phases. The YAG phase results from the reaction between Al_2O_3 and Y_2O_3 additives in the starting powders. The presence of β-SiC could not be previously confirmed in the diffraction pattern, due to the very strong overlap of its Bragg reflections with those of the α-SiC polytypes. However, as the β-SiC polytype is the main constituent of the starting powders we included it in the model used in the refinements. The presence of peaks from polytypes 4H and 6H shows that the β→α transformation takes place during sintering. It is known that β-SiC is unstable over 1600°C in the presence of Al;[34] thus, the sintering of the powders at 1950°C could explain the partial transformation of β-SiC into the α-SiC polytypes 4H and 6H. The different polytypes have small differences in their free energies. Therefore, SiC-based ceramics can contain many polytypes as a mixture of metastable phases. Free energies of α-SiC polytypes are similar to each other, and are much lower than the free energy of β-SiC.[35] Therefore, with sufficient thermal energy, the metastable phase β-SiC transforms to one or more polytypes of α-SiC.

Fig. 3 shows the plot output for the first Rietveld refinement (that corresponding to the true instrumental

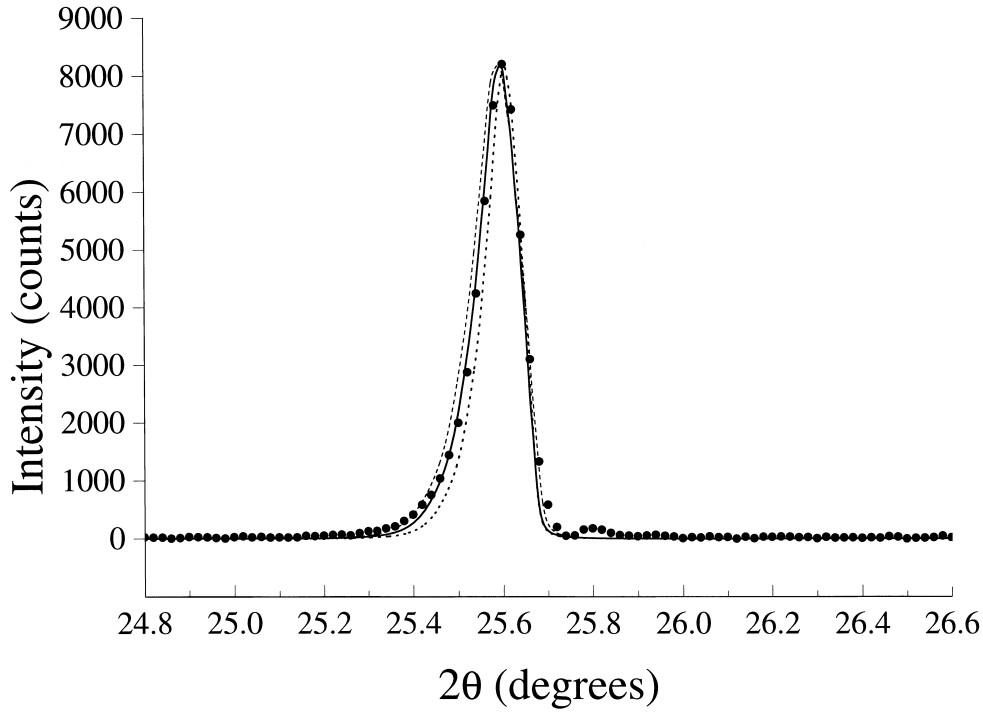

Fig. 1. (012) peak of the α-Al_2O_3 standard sample. Points represent the experimental data, solid line represents the calculated profile according to the true geometrical conditions of the experiment, whereas dotted and dashed lines are the peaks calculated from the narrower and wider instrumental profiles, respectively.

Table 2
Full-width-half-maximum (FWHM) of the true and distorted instrumental profiles at $2\theta = 25.60°$

Instrumental profile	FWHM
True	0.1115°
Narrower	0.0983°
Wider	0.1269°

function), including the difference pattern ($\chi^2 = 4.9$). A cursory look at the other outputs (obtained from the distorted instrumental peaks) does not reveal any difference. Table 3 displays the main results for the three refinements, including quantitative analysis, crystallite size for each phase and agreement indices. We draw attention to two key observations: first, the relative phase proportions are the same, taking into account the experimental errors (about 3%); second, the values of χ^2 and other residuals (R_p and R_{wp}) evaluated by the program remain the same. These facts support the already observed similarity between the three Rietveld plots, and clearly show the insensitivity of the quantitative analysis and the goodness of the refinement to the uncertainty in the starting instrumental function. On the other hand, with increasing/decreasing the width of the instrumental peaks we would expect an increase/decrease of the mean crystallite size, and this is indeed the case. However, the calculated differences are not significant, considering the average uncertainty supplied by the program, except for the β-SiC polytype (the majority phase). This fact can be clarified by resorting to the full overlapping of its Bragg reflections with those of all α-SiC polytypes. In fact, the structure of the α-SiC polytypes can be described on the basis of the cubic close-packed sequence by introducing a suitable and periodic distribution of stacking faults.[36,37]

It is worth noting that, since we have performed an exhaustive characterization of the instrumental effects, we are in position to obtain data concerning crystallite size along a specific crystallographic direction. Moreover, this determination avoids all the complexity of deconvolutions and the well-known difficulties of traditional line-broadening methods. However, a question remains still open: how the mean crystallite size obtained in this way can be compared to that coming from variance, Warren–Averbach and integral breadth methods? A spread within measurements performed by using the above procedures has been reported.[38] We are dealing with systematic differences as long as the variance and Warren–Averbach methods yield a so-called area-weighted value for the crystallite size, whereas the integral breadth method yields a volume-weighted result. Thus, the integral breadth method can easily amount to a value between two and three times the value given by the variance and Warren–Averbach methods.[38,39] Hence, with the aim to clarify this aspect, we have compared the value obtained by using BGMN

for the 4H-SiC polytype (51±6 nm, see Table 2) with that obtained from independent measurements[40] performed by the variance method:[41] 17±3 nm. This seems to indicate that the values supplied by BGMN range between those of the integral breadth method. Such behaviour can be attributed to the way used by the program to calculate this value: the mean crystallite diameter, in a given direction, is evaluated from the Lorentzian contribution to the profile broadening.[17] This is, more or less, the strategy of the integral breadth

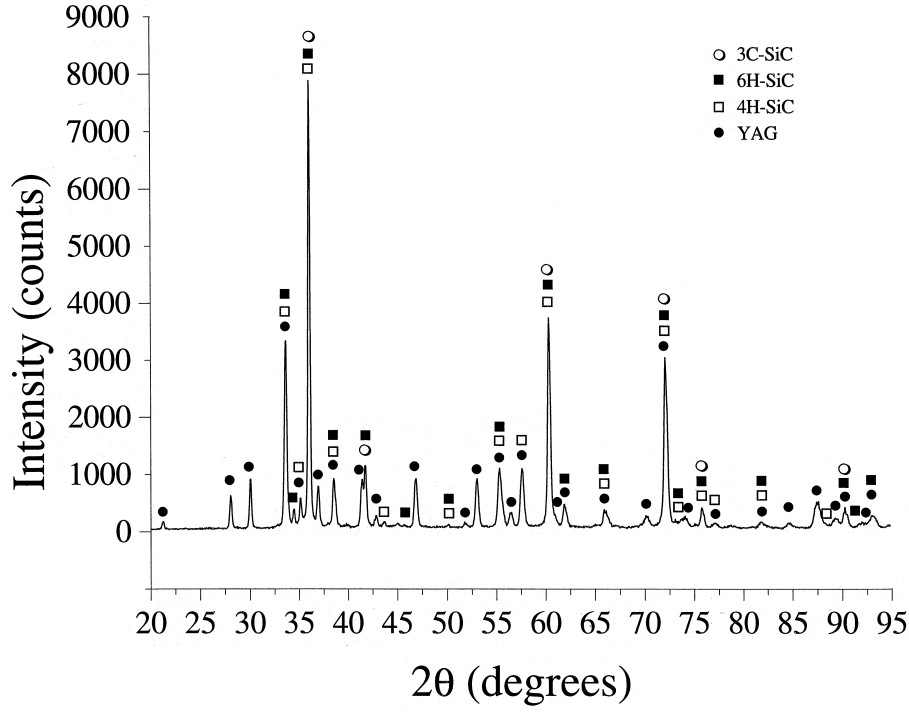

Fig. 2. Powder XRD pattern of the LPS SiC material. The symbols indicate the positions of Bragg reflections of each phase.

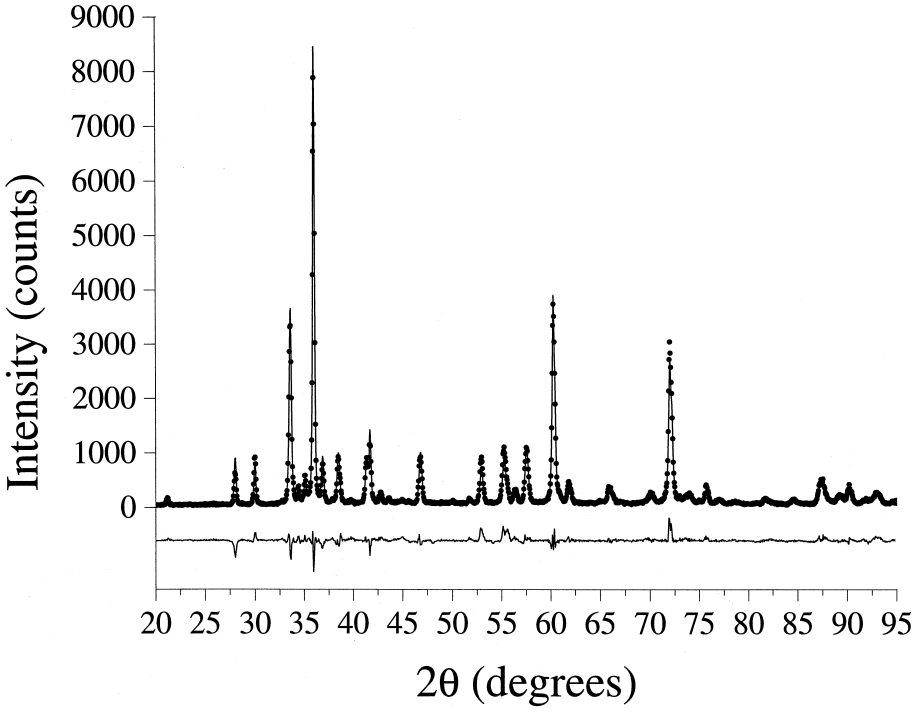

Fig. 3. Rietveld plot obtained by using the true instrumental function. Points represent the observed data and the solid line represents the calculated pattern. The difference plot is shown below.

Table 3
Weight fractions, mean crystallite sizes (nm) and Rietveld agreement indices corresponding to the three instrumental profiles referred in the text

Phase proportions	True profile	Narrower profile	Wider profile
3C (wt%)	47.5 (15)	48.0 (15)	46.9 (14)
4H (wt%)	12.4 (17)	13.1 (17)	12.6 (16)
6H (wt%)	15.4 (12)	13.9 (12)	15.7 (13)
YAG (wt%)	24.7 (4)	24.9 (4)	24.8 (4)
Mean crystallite size along a given direction	True profile	Narrower profile	Wider profile
3C (111)	109 (16)	79 (8)	138 (26)
4H (101)	51 (6)	44 (5)	56 (8)
6H (102)	37 (5)	43 (6)	35 (4)
YAG (420)	55 (4)	49 (3)	58 (5)
Agreement indices	True profile	Narrower profile	Wider profile
R_p	10.3	10.3	10.4
R_{wp}	14.2	14.2	14.4
χ^2_r	4.9	4.9	5.0

method, where the mean size is obtained from the Lorentzian broadening although the knowledge of the Gaussian contribution is essential in order to separate both parts, Lorentzian and Gaussian, from the full integral breadth.

5. Conclusions

The commonly known "fundamental parameters approach" (FPA) has recently set a new trend within the Rietveld method. In this approach, after a preliminary evaluation of the spectral and instrumental sources of broadening, quantitative analysis and crystallite size/strain measurements can be performed without reference to traditional methodologies.

Still more recently, an enthusiastic discussion has been raised among the users of the Rietveld method. In fact, the computation of the instrumental function in FPA is far from being a trivial task, and it is not absolutely free of empiricism (it is nearly impossible to have just zero % of empiricism, at least in our real world). Thus, our goal was to have a quantitative assessment of the agreement between the modelled instrumental profile and that measured on a standard (sieved and well-annealed alumina, in our case). On the basis of a well-known FPA program, BGMN, we have proved the near insensitivity of the main steps of the refinement and quantitative analysis versus simulated inaccuracy of the instrumental function. Obviously, this is not the case for crystallite size measurements, where we have also showed that the results reported are consistent with traditional methods and of the order of that obtained by the integral breadth method.

On the other hand, this kind of experiment was performed on an important structural material: liquid-phase-sintered SiC ceramic. A remarkable aspect of this class of materials is that they can be significantly toughened through careful microstructure design. However, the microstructural evolution in these ceramics remains not well understood because of the $\beta \rightarrow \alpha$ transformation and the significant overlap of the Bragg reflections from the polytypes. Thus, this work contributes to the knowledge of the microstructural evolution by an accurate quantitative analysis and crystallite size determinations of SiC polytypes.

Acknowledgements

The authors thank Mrs. H. Xu and Professor N.P. Padture at University of Connecticut for their experimental assistance. Financial support fot this work was provided by the Consejeria de Educacion y Juventud de la Junta de Extremadura under Grant No. IPR98C016.

References

1. Klug, H. P. and Alexander, L. E., *X-ray Procedures for Polycrystalline and Amorphous Materials*. John Wiley and Sons, New York, 1974 (Chapter 9).
2. Ruska, J., Gauckler, L. J., Lorenz, J. and Rexer, H. U., The quantitative calculation of SiC polytypes from measurements of X-ray diffraction peak intensities. *J. Mater. Sci.*, 1979, **14**, 2013–2017.
3. Frevel, L. K., Petersen, D. R. and Saha, C. K., Polytype distribution in silicon carbide. *J. Mater. Sci.*, 1992, **27**, 1913–1925.
4. Rietveld, H. M., A profile refinement method for nuclear and magnetic structures. *J. Appl. Cryst.*, 1969, **2**, 65–71.
5. Albinati, A. and Willis, B. T. M., The Rietveld method in neutron and X-ray powder diffraction. *J. Appl. Cryst.*, 1982, **15**, 361–374.
6. Bish, D. L. and Howard, S. A., Quantitative phase analysis using the Rietveld method. *J. Appl. Cryst.*, 1988, **21**, 86–91.
7. Dollase, W. A., Correction of intensities for preferred orientation in powder diffractometry: application of the March model. *J. Appl. Cryst.*, 1986, **19**, 267–272.
8. Valvoda, V., Chládek, M. and Cerný, R., Joint texture refinement. *J. Appl. Cryst.*, 1996, **29**, 48–52.

9. Rodríguez-Carvajal, J., FULLPROF: a program for Rietveld refinement and pattern matching analysis. In A*bstracts of the Satellite Meeting on Powder Diffraction of the XV Congress of the IUCr*, Toulouse, France, 1990, p. 127.
10. Larson, A. C. and von Dreele, R. B. Report No. LA-UR-86-748. Los Alamos Laboratory, Los Alamos, USA, 1987.
11. Izumi, F., Rietveld analysis program RIETAN and PREMOS and special applications. In *The Rietveld Method*, ed. R. A. Young. Oxford University Press, Oxford, UK, 1993, (Chapter 13).
12. Hill, R. J., Rietveld refinement round robin. I. Analysis of standard X-ray and neutron data for $PbSO_4$. *J. Appl. Cryst*., 1992, **25**, 589–610.
13. Jorgensen, J. E. and Rasmussen, S. E., Refinement of the structure of MnSi by powder diffraction. *Powder Diffrac*., 1991, **6**, 194–195.
14. Caglioti, G., Paoletti, A. and Ricci, F. P., Choice of collimators for a crystal spectrometer for neutron diffraction. *Nucl. Instrum. Methods*, 1958, **3**, 223–228.
15. Bergmann, J., Kleeberg, R., Taut, T. and Haase, A., Quantitative phase analysis using a new Rietveld algorithm-assisted by improved stability. *Adv. X-ray Anal*., 1997, **40**, 112.
16. *KOALARIET manual user*.
17. *BGMN manual user*.
18. Langford, J. I., The variance and other measures of line broadening in powder diffractometry. I. Practical Considerations. *J. Appl. Cryst*, 1968, **1**, 48–59.
19. Langford, J. I., The variance and other measures of line broadening in powder diffractometry. II. determination of particle size. *J. Appl. Cryst*., 1968, **1**, 131–138.
20. Warren, B. E. and Averbach, B. L., The effect of cold-work distortion on X-ray patterns. *J. Appl. Phys*., 1950, **21**, 595–599.
21. Delhez, R. and Mittemeijer, E. J., The elimination of an approximation in the Warren–Averbach analysis. *J. Appl. Cryst*., 1976, **9**, 233–234.
22. De Keijser, Th.H., Langford, J. I., Mittemeijer, E. J. and Vogels, A. B. P., Use of the voigt function in a single-line method for the analysis of X-ray diffraction line broadening. *J. Appl. Cryst*., 1982, **15**, 308–314.
23. De Keijser, Th.H., Mittemeijer, E. J. and Rozendaal, H. C. F., The determination of crystallite-size and lattice-strain parameters in conjunction with the profile-refinement method for the determination of crystal structures. *J. Appl. Cryst*., 1983, **16**, 309–316.
24. Stokes, A. R., A numerical fourier-analysis method for the correction of widths and shapes of lines on X-ray powder photographs. *Proc. Phys. Soc. London*, 1948, **61**, 382–391.
25. Omori, M. and Takei, H., Pressureless sintering of SiC. *J. Am. Ceram. Soc*., 1982, **65**(6), C92.
26. Negita, K., Effective sintering aids for silicon carbide ceramics: reactivities of silicon carbide with various additives. *J. Am. Ceram. Soc*., 1986, **69**(12), C308–C310.
27. Mulla, M. A. and Krstic, V. D., Low-temperature pressureless sintering of β-silicon carbide with aluminum oxide and yttrium oxide additions. *Am. Ceram. Soc. Bull*., 1991, **70**(3), 439–443.
28. Padture, N. P., In situ-toughened silicon carbide. *J. Am. Ceram. Soc*., 1994, **77**(2), 519–523.
29. Padture, N. P. and Lawn, B. R., Toughness properties of a silicon carbide with *in situ*-induced heterogeneous grain structure. *J. Am. Ceram. Soc*., 1994, **77**(10), 2518–2522.
30. Lee, S. K., Kim, Y. C. and Kim, C. H., Microstructural development and mechanical properties of pressureless-sintered SiC with plate-like grains using Al_2O_3–Y_2O_3 additives. *J. Mater. Sci*., 1994, **29**, 5321–5326.
31. Mulla, M. A. and Krstic, V. D., Mechanical properties of β-SiC pressureless sintered with Al_2O_3 additions. *Acta Metall. et Mater*., 1994, **42**(1), 303–308.
32. Ramsdell, L. S., Studies in silicon carbide. *Am. Min*., 1947, **32**, 64–82.
33. Cumbrera, F. L., Sánchez-Bajo, F., Fernández, R. and Llanes, L., Microstructure effects in the X-ray powder diffraction profile of 9 mol% Mg-PSZ. *J. Eur. Ceram. Soc*., 1998, **18**, 2247–2252.
34. Jepps, N. W. and Page, T. F., Polytypic transformations in silicon carbide. *Prog. Cryst. Growth Charact*., 1983, **7**, 259–307.
35. Heine, V., Cheng, C. and Needs, R. J., A computational study into the origin of SiC polytypes. *Mater. Sci. Eng. B*, 1992, **11**, 55–60.
36. Pujar, V. V. and Cawley, J. D., Computer simulations of diffraction effects due to stacking faults in β-SiC: I. Simulation results. *J. Am. Ceram. Soc*., 1997, **80**, 1653–1662.
37. Xu, H. Microstructural Evolution in *In-Situ* Reinforced Silicon Carbide: The effect of Starting Powder. MS thesis, University of Connecticut, 1999.
38. Sánchez-Bajo, F., Cumbrera, F. L., Guiberteau, F., Domínguez-Rodríguez, A. and Tsodikov, M. V., X-ray microstructural characterization of Y-PSZ (5 mol%) nanocrystalline powder samples. *Mater. Lett*., 1998, **33**, 283–289.
39. Sánchez-Bajo, F., Caracterización microestructural del sistema Y-PSZ. PhD thesis, University of Extremadura, 1993.
40. Ortiz, A. L., Aplicación del método de Rietveld al estudio de la transformación β→α en policristales de SiC sinterizados en fase líquida. MS thesis, University of Extremadura, 1999.
41. Sánchez-Bajo, F. and Cumbrera, F. L., The use of the pseudo-Voigt function in the variance method of X-ray line-broadening analysis. *J. Appl. Cryst*., 1997, **30**, 427–430.